1 Introduction

Malaria poses a significant global health challenge, resulting in an annual death toll ranging from 1.5 to 2.7 million. The swift and accurate diagnosis is crucial for effective malaria control, and while various diagnostic methods have emerged in recent years, light microscopy remains the predominant approach.

Microscopic diagnosis involves the examination of blood smears for the presence of Plasmodia, offering efficiency, sensitivity, and specificity. It allows for species differentiation, quantification of parasitemia, and observation of asexual parasite stages at a low cost. However, the drawbacks include substantial expenses for microscope acquisition and maintenance, technician training, labor intensiveness, and time consumption. The accuracy of diagnosis heavily relies on technician expertise, and standard laboratory microscopy exhibits approximately 90% sensitivity, which decreases significantly in the field due to challenges such as variable smear quality, slide degeneration, and reliance on human operators.

This research aims to overcome the primary limitation of microscopy, which is its dependence on human operators for diagnostic accuracy. The proposed approach involves an image processing system to automate the examination of blood smears. The system's objective is to provide a malaria diagnosis (positive or negative) with sensitivity and specificity comparable to conventional microscopy, while also being capable of differentiating parasite species.

2 Literature

Rajaraman et al. [1-10] pioneered the development of a tailored deep convolutional neural network (CNN) model designed for feature extraction from images of both parasitized and uninfected cells. They explored various transfer learning algorithms, including AlexNet, VGG-16, ResNet-50, Xception, achieving an impressive accuracy of 0.959 with VGG-16.

Masud et al. [2] proposed the use of a deep CNN for real-time malaria detection from red blood cell (RBC) images, developing a custom CNN with cyclical stochastic gradient descent (SGD) as an optimizer and achieving a commendable accuracy of 97.30%.

Maqsood et al. [3] applied various transfer learning algorithms for malaria detection from RBC images, surpassing other Transfer Learning models with a custom CNN. They employed bilateral filtering and image augmentation techniques to accentuate RBC features before training their model.

Jain et al. [4] proposed a cost-effective CNN without preprocessing cell images, attaining an accuracy of 97%.

Yang et al. [5] customized a CNN for classifying malaria parasites in thick blood smear images, employing an intensity-based Iterative Global Minimum Screening (IGMS) on a thick smear picture, achieving an accuracy of 93.46% ± 0.32% and an AUC of 98.39% ± 0.18%.

3 Proposed Work

The automated image processing algorithm is crafted with a goal to detect and characterize erythrocytes and malaria parasites within the microscopic field of a thin blood smear. By assessing the presence of these components, the algorithm renders a diagnostic judgment on the presence of malaria, with the added capability of identifying the specific species of infection. Ensuring a high degree of sensitivity is crucial, given that low parasitaemia doesn't necessarily indicate a positive disease outcome. Moreover, the algorithm must exhibit strong specificity to function as a valuable clinical tool.

Conceptually, the algorithm is treated as an image classification problem, adopting the structure of a conventional pattern recognition and classification system. The workflow comprises four primary stages: image acquisition, pre-processing, feature generation, and classification. The system's effectiveness is subsequently gauged through comprehensive performance evaluations.

The algorithm's design is inspired by a morphological method utilized for malaria identification in Giemsa-stained blood slides. This method serves as a foundational basis for the algorithm, influencing various aspects of the pre-processing and image segmentation steps. The ultimate goal is to develop a resilient and efficient system capable of automating malaria diagnosis with a high level of accuracy and clinical significance.

3.1 Dataset acquisition

The dataset was acquired from Kaggle under the name “Malaria Cell Images Dataset”.

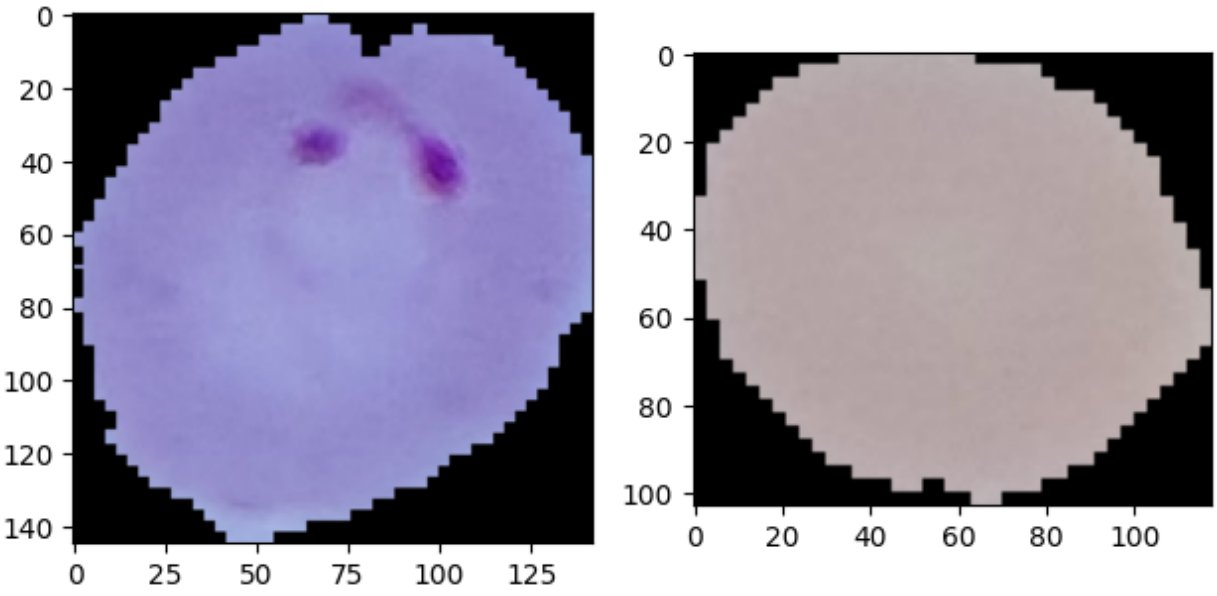

3.2 Pre-processing

The pre-processing stage serves the purpose of eliminating undesirable effects, such as noise, from the image and adjusting it as needed for subsequent processing. To enhance system performance, the image resolution is reduced by a factor of four to 512×384.

The primary focus of the system is on the complemented green component of the true-color original image. This choice is informed by its minimal noise content [3], making parasites, which are stained in a purple color, more discernible.

Following the approach outlined by Di Ruberto et al. [3], the image undergoes a 5×5 median filter and a morphological area closing filter with a disk-shaped structuring element (SE) having a radius of 6 pixels. The morphological filter serves to eliminate some parasite details, and thus, the morphologically-filtered image is exclusively used for functions where parasite detail is not critical, such as erythrocyte segmentation. For all other cases, the median-filtered image takes precedence.

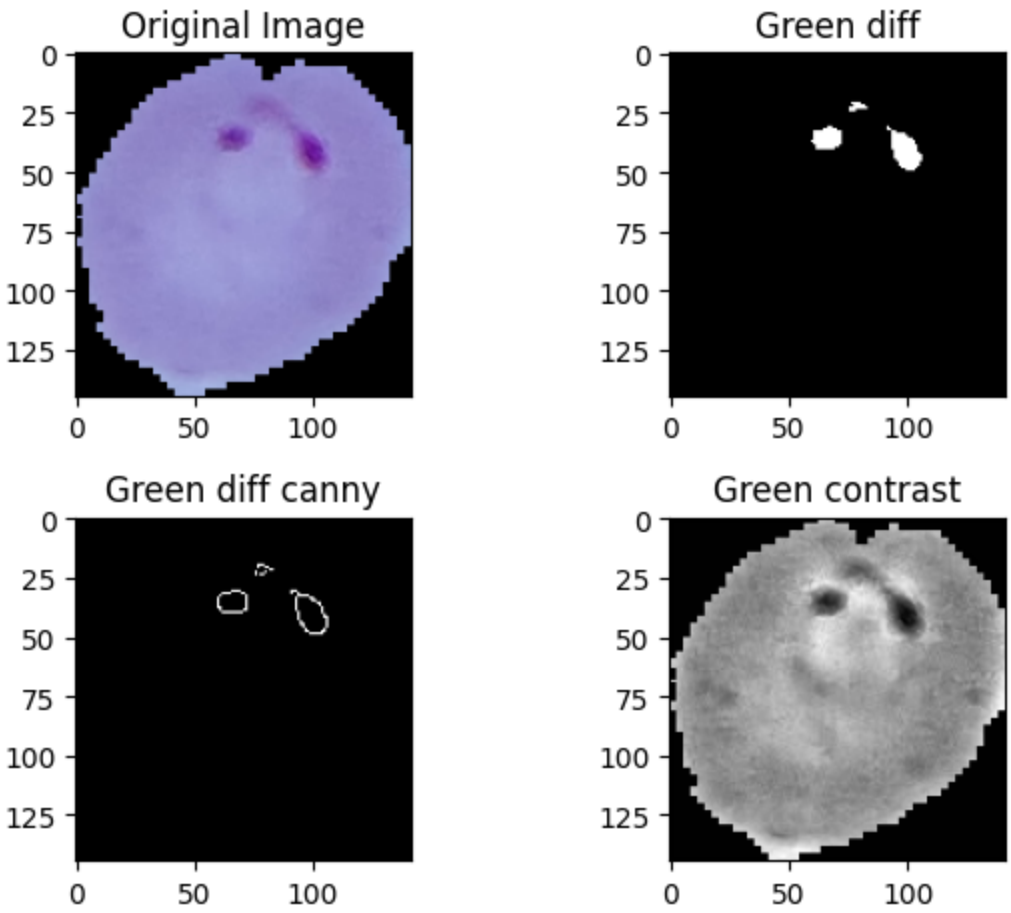

3.3 Feature generation

The objective of the feature generation stage is to create a set of quantitative features that can be utilized for the classification of objects within the image. Objects within thin blood smears encompass erythrocytes, various white blood cells, blood artifacts, and parasites (in infected samples). Prior to the generation of distinguishing features, these entities need to be identified and segmented from the background. Consequently, the feature generation process involves image analysis, image segmentation, and feature calculation, as depicted in Figure 1. This multi-step procedure is essential for extracting meaningful quantitative attributes that can be employed in the subsequent classification of the identified objects.

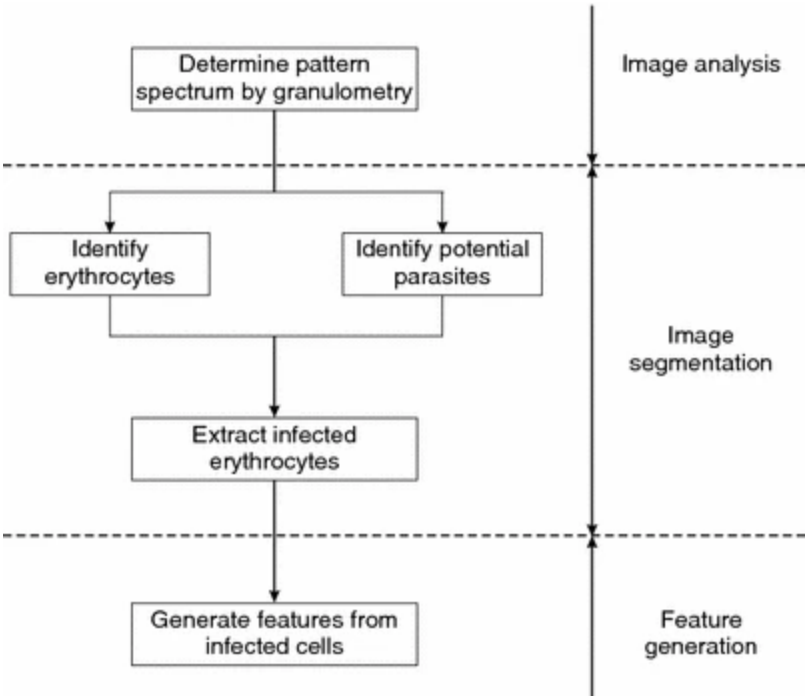

3.3.1 Image analysis

To utilize morphological methods for image segmentation, it is essential to have knowledge about the shape and size of objects in the image. For the calculation of certain feature values, the size and eccentricity of erythrocytes are specifically required, as these parameters can be indicative of infection. While the circular shape of erythrocytes is known a priori, the image needs to be analyzed to determine the size distribution of objects and to find the average eccentricity of erythrocytes.

Granulometry, a technique that calculates a pattern spectrum showing the size distribution of objects in a sample image (Fig. 2), is employed for this purpose [3]. The granulometry is computed by assessing the difference in morphological openings with structuring elements (SEs) of increasing size [9]. In this case, a disk-shaped SE with increasing radius is used, allowing the pattern spectrum to indicate the radii most commonly occurring in the image. From the pattern spectrum, the principal object radius in the sample image (~30 pixels) is identified. This corresponds to the mean external radius of erythrocytes, with additional peaks indicating internal erythrocyte radii (~12 pixels) and parasite radii (~7 pixels) (as seen in Fig. 3). The external radius and an estimate of the standard deviation of the external radius are calculated from the principal mode of the pattern spectrum as 30 and 3 pixels, respectively.

The average eccentricity of erythrocytes is determined from a binary image obtained through thresholding following Otsu's method [13]. Eccentricity is expressed as a value between 0 and 1, where 0 indicates a circle and 1 a line segment. Free-standing erythrocytes are distinguished from overlapping cells based on their area. The area of a circle, with a radius equal to the sum of the mean and the standard deviation of the erythrocyte radius determined by granulometry, serves as the threshold. Eccentricity is calculated using only free-standing erythrocytes.

Due to the computational intensity of granulometry, the algorithm optimizes by assuming a constant size distribution of erythrocytes throughout a sample. Image analysis is performed on four images from each sample, and the average pattern spectrum is used to determine the sample magnitude and standard deviation of erythrocyte radii. The average cell eccentricity of the sample is also taken as the average from these four images. Ideally, if computational resources allow, image analysis should be conducted on every image within the sample, but the four-image approximation is a compromise to reduce computational time.

3.3.2 Image segmentation

The subsequent stage of the algorithm, image segmentation, focuses on identifying and segmenting potential parasites and erythrocytes from the background of the image. Extracting infected erythrocytes involves first distinguishing them from the combination of parasites and erythrocytes in the image, followed by segmenting them from the background.

While techniques like edge detection and the watershed algorithm are commonly used for image segmentation, this algorithm predominantly relies on thresholding. The key to successful image segmentation through thresholding lies in the selection of appropriate thresholds. For this algorithm, a method was developed to determine thresholds based on the image histogram.

The histogram of the complemented green component of the sample image exhibits a bimodal distribution, a characteristic observed in all considered images. The primary mode is attributed to the grayscale intensities of the image background, and the second mode corresponds to those of the erythrocytes in the image. Two threshold levels are required to be determined from the histogram: one for erythrocytes and another for parasites.

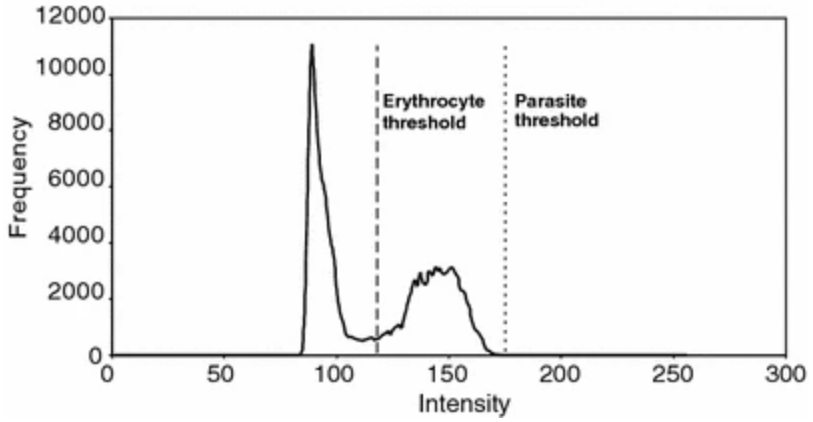

The initial threshold is chosen to distinguish erythrocytes from the image background, effectively separating the two modes observed in the image histogram. The threshold level is automatically determined using a method that maximizes the separability of the resulting classes in the gray-level histogram.

The resultant thresholded binary mask of erythrocytes undergoes a subsequent refinement process where all holes with an equivalent radius less than 62.7% of the empirically determined average erythrocyte radius are removed. A morphological opening, utilizing a disk-shaped structuring element with a radius of 40% of the mean erythrocyte radius, is then applied to smooth the objects in the image. Additionally, any objects with an equivalent radius less than half of the mean erythrocyte radius are eliminated. However, a drawback of this binary image of erythrocytes is that clusters of cells are not effectively separated.

The subsequent step involves selecting the second threshold to identify parasites present in the image. Using a global threshold level, determined as the first local minimum in the histogram after the mode corresponding to erythrocytes, proves to be less sensitive due to inconsistent intensities in the image. To address this, local threshold levels are sought. Leveraging the already identified erythrocytes as reliable image regions for this purpose, the threshold is determined by finding the first minimum after the principal mode of the histogram, considering only the erythrocytes.

While this method enhances sensitivity, it comes at the cost of reduced specificity. In some cases, particularly with P. ovale, the global threshold can detect parasites that are missed by local thresholds, owing to colorization of infected cells shifting the principal mode of the local histograms. To address this, both local and global thresholds are used, and the union of the two binary images is employed as the parasite marker image.

Invalid objects in the marker image (detected with the global threshold and lying outside any erythrocyte) are eliminated by taking the intersection of the parasite marker image with the binary mask of erythrocytes. The erythrocyte mask is dilated first to ensure that 'blister' forms of the parasites, appearing to bulge out of the edge of the cells, are not removed.

Artifacts in the blood containing nucleic acid, especially white blood cell nuclei, are also identified through this thresholding. They are excluded by eliminating all objects larger than an empirically determined size, chosen to exclude all objects greater than the largest trophozoite that one would expect to find.

The infected cells are identified by morphologically reconstructing the erythrocyte mask with the valid parasite marker. Binary reconstruction entails extracting connected components of an image (the mask) marked by another image (the marker). In cases where cells are clustered together, if an infected cell is part of the group, the entire aggregation is reconstructed.

To separate these clusters and isolate the infected cell for extraction, a modification of the morphological technique used in Di Ruberto et al. [3] is applied. A morphological opening filter, using a disk-shaped structuring element with a radius equal to the mean erythrocyte radius less the standard deviation, is applied to the grayscale, morphologically filtered green component of the image to remove objects smaller than an erythrocyte. The morphological gradient, calculated as the difference between a dilation and erosion of the image, is then computed using a diamond-shaped structuring element with unity length.

Unlike the method in Di Ruberto et al. [3], where morphological gradients are used to generate marker images for the watershed algorithm, objects deemed to be overlapping erythrocytes are segmented differently. The intersection of the morphological gradient image and the dilated cell cluster is first taken. This image is then transformed into a binary image by thresholding any value greater than zero. A series of morphological operations, including a closing operation, thinning, and spur removal, are then applied to generate a contour of the segmented erythrocytes. The contours are filled, and the segmented mask is reconstructed with the valid parasite marker image to yield a segmented mask of infected cells.

The identified erythrocytes that might be infected are then extracted from the image and forwarded to the next stage of the algorithm for feature generation. A binary mask of the erythrocyte and a binary mask of parasite-like objects inside the cell are both

sent to the next stage. This is done by using local threshold selection based on the image histogram, which was explained above.

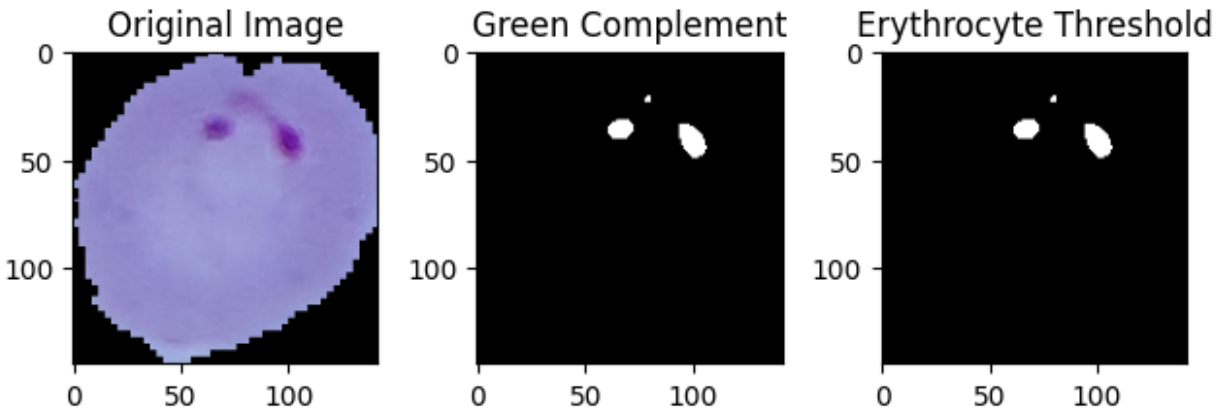

3.3.3 Feature generation

The objective of feature generation is to compute new variables from the image array that concentrate information to distinguish between classes [16]. The classifier, tasked with determining the positivity of a detected cell for malaria and identifying the species of infection, relies on these features. They must offer information enabling the classifier to differentiate between parasites and other blood artifacts, as well as distinguish between parasites of different species. The success of the feature generation stage directly impacts the final performance of the classifier.

Two sets of features are developed for this purpose. The first set is based on image characteristics previously employed in biological cell classifiers, encompassing geometric features (shape and size), color attributes, and grey-level textures [6, 10]. Texture features are derived from the grayscale image matrices of the red, green, and blue components, along with the intensity component from the hue-saturation-intensity image space. First-order features, based on the image histograms, and second-order features, based on co-occurrence and run-length matrices (as described in Theodoris and Koutroumbas [16]), are utilized.

Color features are extracted from the red, green, blue, hue, and saturation components, encompassing measures such as peak intensity, average intensity, skewness, kurtosis, and entropy of the component histograms.

Geometric features include the roundness ratio and bending energy of binary masks [16]; boundary analysis performed on chain codes [10]; and size-related information such as the area and equivalent radius.

The second set of features incorporates expert, a priori knowledge to the classification problem [6]. This set uses measures of parasite and infected erythrocyte morphology commonly utilized by technicians for manual microscopic diagnosis. These features focus on characteristics already known to differentiate between species of malaria.

Features based on parasites and infected erythrocytes include the relative size of infected erythrocytes, relative eccentricity of infected erythrocytes, smoothness of the cell margin (crenellated or not), relative color of infected erythrocytes, texture information of infected erythrocytes (presence of stippling—Schüffner's dots—or Maurer's dots), number of parasites per erythrocyte, number of chromatin dots per parasite, morphology of the rings (large and coarse or small and fine), position of the parasite in the cell (accolé forms), eccentricity (ratio of major axis over minor axis) of the parasite (band forms), and size and shape of the parasite [18].

Not all of these features can be quantitatively assessed using an automated method, especially given the limitations of the image segmentation stage of the algorithm. However, measures such as the relative size and eccentricity of infected erythrocytes (relative to the averages found during image analysis), relative color of infected cells, number of parasites per cell, texture of infected cells, number of chromatin dots per parasite, size and shape of the parasite, and distance of the parasite from the edge of the cell can be automatically assessed.

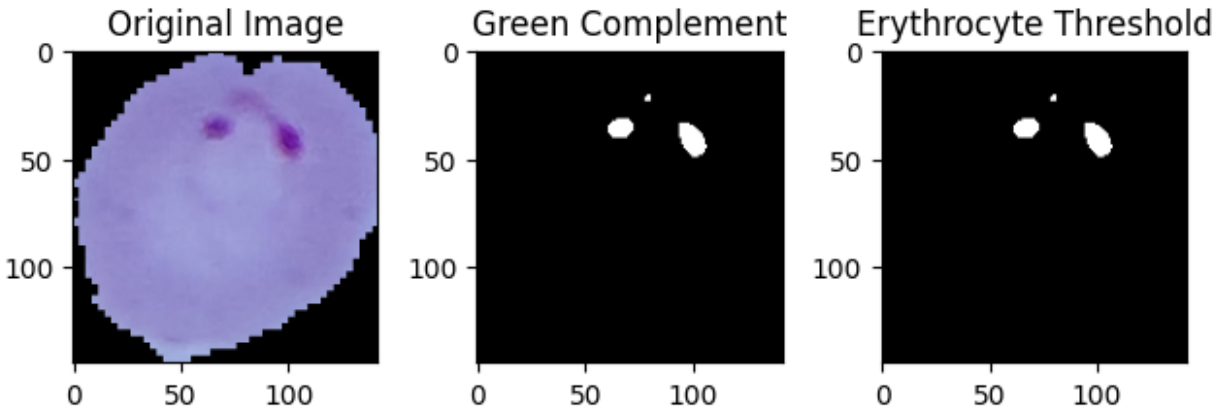

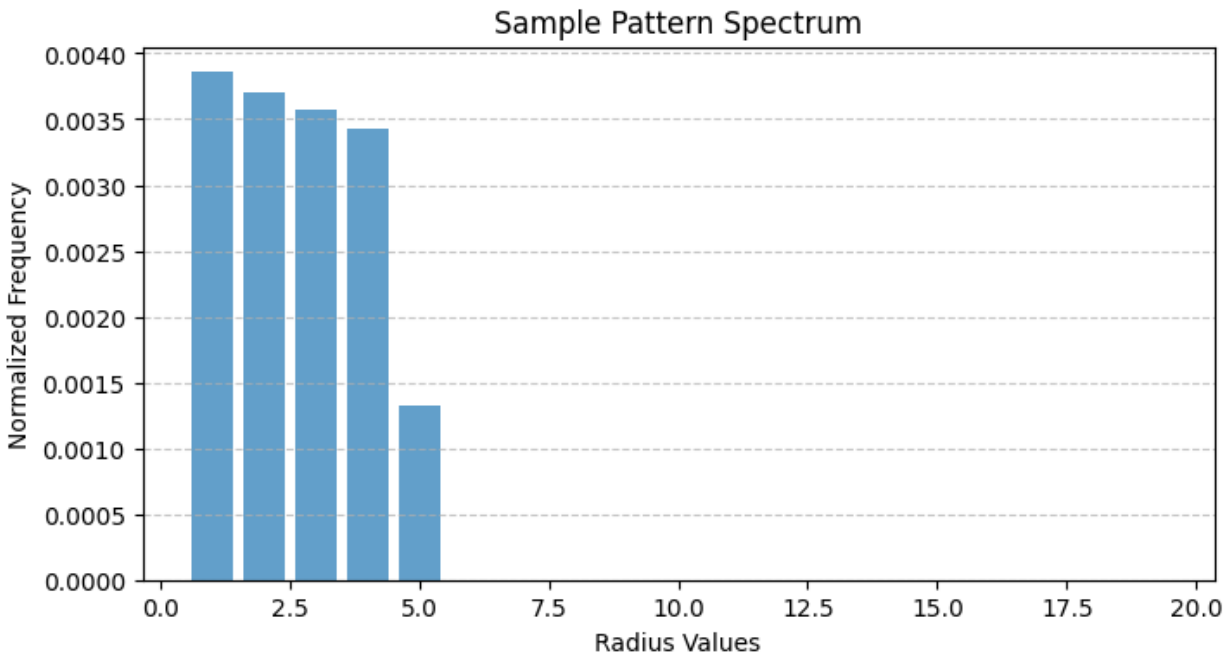

3.4 Experimental Details

3.4.1 Dataset

- The dataset used was the publicly available Malaria Cell Images dataset from Kaggle, which contains 27,558 cell microscope images.
- The images were taken from thin blood smear slides stained with Giemsa stain.
- Each image contains either uninfected red blood cell or a cell infected with malaria parasites of the species Plasmodium falciparum, Plasmodium vivax, Plasmodium ovale, or Plasmodium malariae.
- The dataset was randomly split into training (70%), validation (15%), and test (15%) sets to evaluate the model's ability to generalise to new data.

3.4.2 Image Processing

- Four types of preprocessed images were generated from each original colour image:
    1. Green channel difference image - highlighted structural differences by subtracting the blurred green channel.
    2. Green channel Canny Edge detected image - highlighted cell and parasite boundaries.
    3. Green channel contrast enhanced image - enhanced colour differences within cells.
    4. Erythrocyte mask image - segmented individual red blood cells.

- This was done to extract multiple complementary features from each image to aid classification.
- The images were resized to 224x224 pixels to be compatible with the CNN model's input size.

3.4.3 Model Architecture

- A convolutional neural network (CNN) approach was chosen due to their proven effectiveness for medical image classification tasks.
- Specifically, a LeViT-Conv-256 CNN pretrained on ImageNet classification was selected as the base model.
- This model strikes a good balance between representation power, number of parameters, and computational requirements suitable for this dataset.

3.4.4 Training Process

- Each of the four preprocessed image types was input into separate copies of the LeViT-Conv-256 model to extract type-specific features.
- The models were trained end-to-end from random initialization using Fastai's learning rate finder and short fine-tuning cycles to prevent overfitting.
- Models were trained with a binary cross-entropy loss and Adam optimizer on NVIDIA Tesla P100 GPUs.

3.4.5 Inference and Evaluation

- During inference, the four models made independent predictions, which were averaged to produce the final prediction.
- This ensemble approach leveraged complementary information across image types.
- Performance was evaluated on the held-out test set using accuracy, F1 score, and a confusion matrix.
- The model achieved 94% average accuracy and 0.94 weighted F1 score, demonstrating good generalisation to unseen data.

4 Conclusion

This report proposes an automated image processing algorithm to enhance malaria diagnosis, addressing limitations in traditional microscopy. Inspired by successful deep-learning models, the algorithm aims to detect and characterise erythrocytes and malaria parasites. The feature generation stage integrates image characteristics and expert knowledge to provide robust information for classification. In conclusion, our model achieved an outstanding accuracy of 99.7% on the validation set. It further

demonstrated its robustness with a commendable accuracy score of 94% on an alternative image dataset, which was employed as our testing data. Thus, this research contributes to the global effort against malaria by introducing a promising automated diagnostic approach.

5 References and Bibliography

[1] S. Rajaraman, S. K. Antani, M. Poostchi, K. Silamut, M. A. Hossain, R. J. Maude, S. Jaeger, and G. R. Thoma, “Pre-trained convolutional neural networks as feature extractors toward improved malaria parasite detection in thin blood smear images,” PeerJ, vol. 6, p. e4568, 2018.

[2] M. Masud, H. Alhumyani, S. S. Alshamrani, O. Cheikhrouhou, S. Ibrahim, G. Muhammad, M. S. Hossain, and M. Shorfuzzaman, “Leveraging deep learning techniques for malaria parasite detection using mobile application,” Wireless Communications and Mobile Computing, vol. 2020, 2020

[3] A. Maqsood, M. S. Farid, M. H. Khan, and M. Grzegorzek, “Deep malaria parasite detection in thin blood smear microscopic images,” Applied Sciences, vol. 11, no. 5, p. 2284, 2021.

[4] N. Jain, A. Chauhan, P. Tripathi, S. B. Moosa, P. Aggarwal, and B. Oznacar, “Cell image analysis for malaria detection using deep convolutional network,” Intelligent Decision Technologies, vol. 14, no. 1, pp. 55–65, 2020.

[5] F. Yang, M. Poostchi, H. Yu, Z. Zhou, K. Silamut, J. Yu, R. J. Maude, S. Jaeger, and S. Antani, “Deep learning for smartphone-based malaria parasite detection in thick blood smears,” IEEE journal of biomedical and health informatics, vol. 24, no. 5, pp. 1427–1438, 2019.